The Stereochemistry of 1,2,3-Triols Revealed by H-1 NMR Spectroscopy: Principles and Applications

ARTICLE *in* CHEMISTRY - A EUROPEAN JOURNAL · NOVEMBER 2009

Impact Factor: 5.73 · DOI: 10.1002/chem.200901505 · Source: PubMed

4 AUTHORS, INCLUDING:

Félix Freire
University of Santiago de Compostela
32 PUBLICATIONS **509** CITATIONS
SEE PROFILE

Enrique Lallana Ozores
The University of Manchester
13 PUBLICATIONS **396** CITATIONS
SEE PROFILE

Ricardo Riguera
University of Santiago de Compostela
252 PUBLICATIONS **5,952** CITATIONS
SEE PROFILE

DOI: 10.1002/chem.200901505

The Stereochemistry of 1,2,3-Triols Revealed by ^{1}H NMR Spectroscopy: Principles and Applications

Félix Freire, Enrique Lallana, Emilio Quiñoá, and Ricardo Riguera*[a]

Abstract: The conformational compositions of the tris(α-methoxy-α-phenylacetic acid) ester derivatives of 1,2,3-*prim*,*sec*,*sec*-triols are presented. These conformations have been determined by theoretical and experimental data (i.e., energy- and chemical-shift calculations, circular dichroism (CD) experiments, coupling-constant analysis, enantioselective deuteration experiments, and low-temperature NMR spectroscopic studies). A detailed analysis of the anisotropic effects due to the most significant conformers in the ^{1}H NMR spectra supported the correlation between the ^{1}H NMR spectra ($\Delta\delta^{RS}$ value of H(3′) and $|\Delta(\Delta\delta^{RS})|$ parameters) and the absolute configuration of the substrate. The study also allows the identification of the *pro-R* and *pro-S* methylene protons from their vicinal coupling constants and relative chemical shifts.

Keywords: alcohols · configuration determination · conformation analysis · methoxyphenylacetic acid · NMR spectroscopy

Introduction

The assignment of the absolute configuration of monofunctional compounds by NMR spectroscopic analysis is now a well-established procedure due to its simplicity, reliability, and convenience. In practice, this technique often requires the preparation of two derivatives of the substrate (e.g., a secondary alcohol) with the *R* and *S* enantiomers of an appropriate auxiliary reagent (e.g., α-methoxy-α-phenylacetic acid) and the comparison of the NMR spectra of the resulting diastereomeric derivatives (Figure 1). These spectra reflect the selective aromatic shielding effects produced by the auxiliary on both substituents of the original substrate (L^1 and L^2), thus revealing the information needed to make the assignment of its configuration.

This procedure was originally reported by Mosher in his pioneering work by using α-methoxy-α-trifluorophenylacetic acid (MPTA) as the chiral auxiliary reagent (the so-called Mosher method)[1] and was further revised and used by others.[2] Over the last few decades, the use of this methodology has expanded a great deal.[3] The development of new and more efficient auxiliary reagents has been reported and the assignment of several families of monofunctional substrates has been achieved (e.g., cyanohydrins, β-hydroxy acids, thiols, alcohols, amines, and carboxylic acids).[3,4] In addition, the experimental procedure has been simplified and optimized with significant achievements, including the possibility of using a single derivative by modification of the temperature of the NMR probe[5] or by selective complexation[6] and the use of auxiliary reagents linked to a resin.[7]

More recently, attention has been focused on the assignment of the absolute configuration of polyfunctional com-

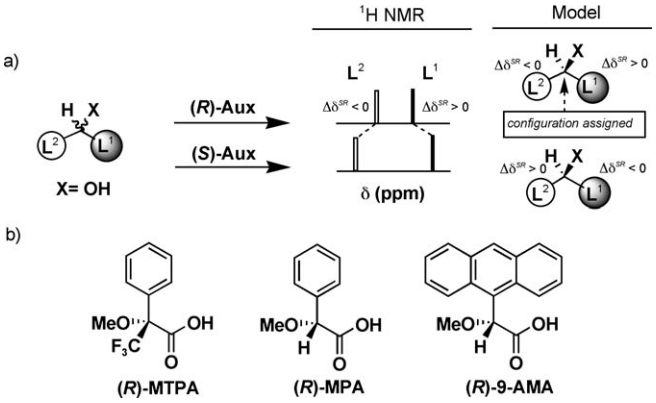

Figure 1. a) General procedure to assign the absolute configuration of secondary alcohols by NMR spectroscopic analysis. b) Structures of the most frequently used arylmethoxyacetic acids. AMA = 9-anthrylmethoxyacetic acid, L = substituent.

[a] Dr. F. Freire, E. Lallana, Prof. Dr. E. Quiñoá, Prof. Dr. R. Riguera
Department of Chemistry
University of Santiago de Compostela
Avd. Ciencias s/n. E-15782 (Spain)
Fax: (+34) 981-591-091
E-mail: ricardo.riguera@usc.es

Supporting information for this article is available on the WWW under http://dx.doi.org/10.1002/chem.200901505.

pounds. The determination of every chiral center is carried out in a single experiment, thus avoiding tedious selective protection/deprotection steps of the different functional groups and making the whole process as simple as possible. The theory behind a model that is valid for the assignment of polyfunctional compounds differs from those for monofunctional systems because it is necessary to have knowledge of the combination of the shielding/deshielding effects produced by each of the auxiliaries on the different substituents of the original substrate. In a similar vein, methods to determine the absolute configuration of difunctional compounds, such as diols[8] and amino alcohols,[9] have been reported. A step forward in this field involves the application of this methodology to trifunctional compounds with 1,2,3-*prim*,*sec*,*sec*-triols as interesting substrates and α-methoxy-α-phenylacetic acid (MPA) an appropriate auxiliary reagent for this study (Figure 2). This structural fragment is found very

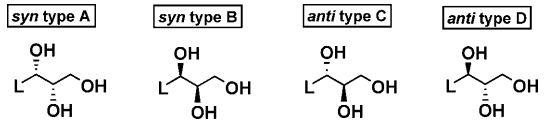

Figure 2. The four diastereoisomers of 1,2,3-*prim*,*sec*,*sec*-triols.

frequently in nature (e.g., sugars and itols amongst others) and in many compounds of pharmaceutical and biological interest, such as Zanamivir (Relenza), sialic acid derivatives, polyoxamic acids, and sphingofungin components. Furthermore, a number of synthetic methods to obtain these triols have been reported.[10]

Although the empirical behavior of the tris-MPA esters of 1,2,3-*prim*,*sec*,*sec*-triols has been discussed,[11] an explanation for this behavior remains unreported. Thus, we decided to study the origins and foundations of the observed experimental data through a description of the most relevant NMR conformers of the tris-MPA ester derivatives and the anisotropic effects associated with these conformations. The overall aim was to rationalize the relationship between the absolute configuration and the ^{1}H NMR spectra.

The $\Delta\delta^{RS}$ parameters from the tris-MPA ester derivatives of 24 triols **1**–**24** of known absolute configuration were taken as the starting point (Figure 3). A summary of these empirical results shows that in those derivatives that resulted from *syn* triols **1**–**12** and **24** the $\Delta\delta^{RS}$ values for H(3′) have the same sign within each configuration (positive in *syn* type A and negative in *syn* type B) and these values are very close in magnitude to those of the corresponding $\Delta\delta^{RS}$ value for H(2′). In those derivatives that result from *anti* triols (**13**–**24**), the $\Delta\delta^{RS}$ values for H(3′) also have the same sign within each configuration (negative in *anti* type C and positive in *anti* type D), but in this case the values of $\Delta\delta^{RS}$ for H(3′) and H(2′) differ to a much larger extent than those protons in the *syn* configuration. Therefore, a correlation exists between the absolute configuration and two experimental NMR spectroscopic parameters: $\Delta\delta^{RS}$ and $|\Delta(\Delta\delta^{RS})|$.

The explanation for this behavior was unveiled by the studies described below and constitutes the first example of configurational assignment by NMR spectroscopic analysis in which the combination of the anisotropic effects of three auxiliaries is presented.

Results and Discussion

Main conformers in the tris-MPA esters of 1,2,3-*prim*,*sec*, *sec*-triols: As mentioned previously, most of the NMR spectroscopic methods used to determine the absolute configuration of chiral compounds are based on the derivatization of the substrate with the two enantiomers of an appropriate auxiliary reagent. The two resulting diastereomeric derivatives must have a well-defined conformational composition (both at the substrate and auxiliary moieties) to enable the correlation between the chemical shifts and the configuration of the substrate. In the case of tris-MPA esters of 1,2,3-*prim*,*sec*,*sec*-triols, it is possible to obtain information about the nature of the most representative conformers by performing an appropriately selected combination of theoretical and experimental studies. The most relevant conformational processes in these compounds are the rotations around the Cα–CO bond of the auxiliary and the rotations around the C(1′)–C(2′), C(2′)–C(3′), and O–C(1′) bonds of the triol (Figure 4).

The rotation around the Cα–CO bond was studied by circular dichroism (CD) spectroscopy. Analysis of the vicinal coupling constants and enantioselective deuteration experiments of the methylene protons were employed to study the rotation around the C(1′)–C(2′) bond. For the other two conformational processes, that is, the rotation around the O–C(1′) and C(2′)–C(3′) bonds, theoretical calculations were performed (DFT at the level B3LYP). In addition, theoretical chemical-shift calculations (gauge including atomic orbital (GIAO)) were carried out. Finally, experimental evidence for all the conformations in solution was obtained by studying the evolution of the NMR spectra with temperature.

The conformational preference around the Cα–CO bond: CD spectroscopic studies: The use of CD spectroscopy was previously described in a study of the conformational equilibrium around the Cα–CO bond in the (*R*)- and (*S*)-MPA esters of secondary alcohols consisting of the more-populated *sp* conformer (i.e., coplanar methoxy and carbonyl groups) and the less-populated *ap* conformer (i.e., antiperiplanar methoxy and carbonyl groups).[12] These systems gave rise to negative and positive CD bands for the (*R*)- and (*S*)-MPA ester derivatives, respectively. An analogous conformational composition was also reported for the MPA esters of 1,2-diols (both secondary/secondary and primary/secondary) and chiral primary alcohols in the α position,[8a–d] as the same CD band patterns were obtained.

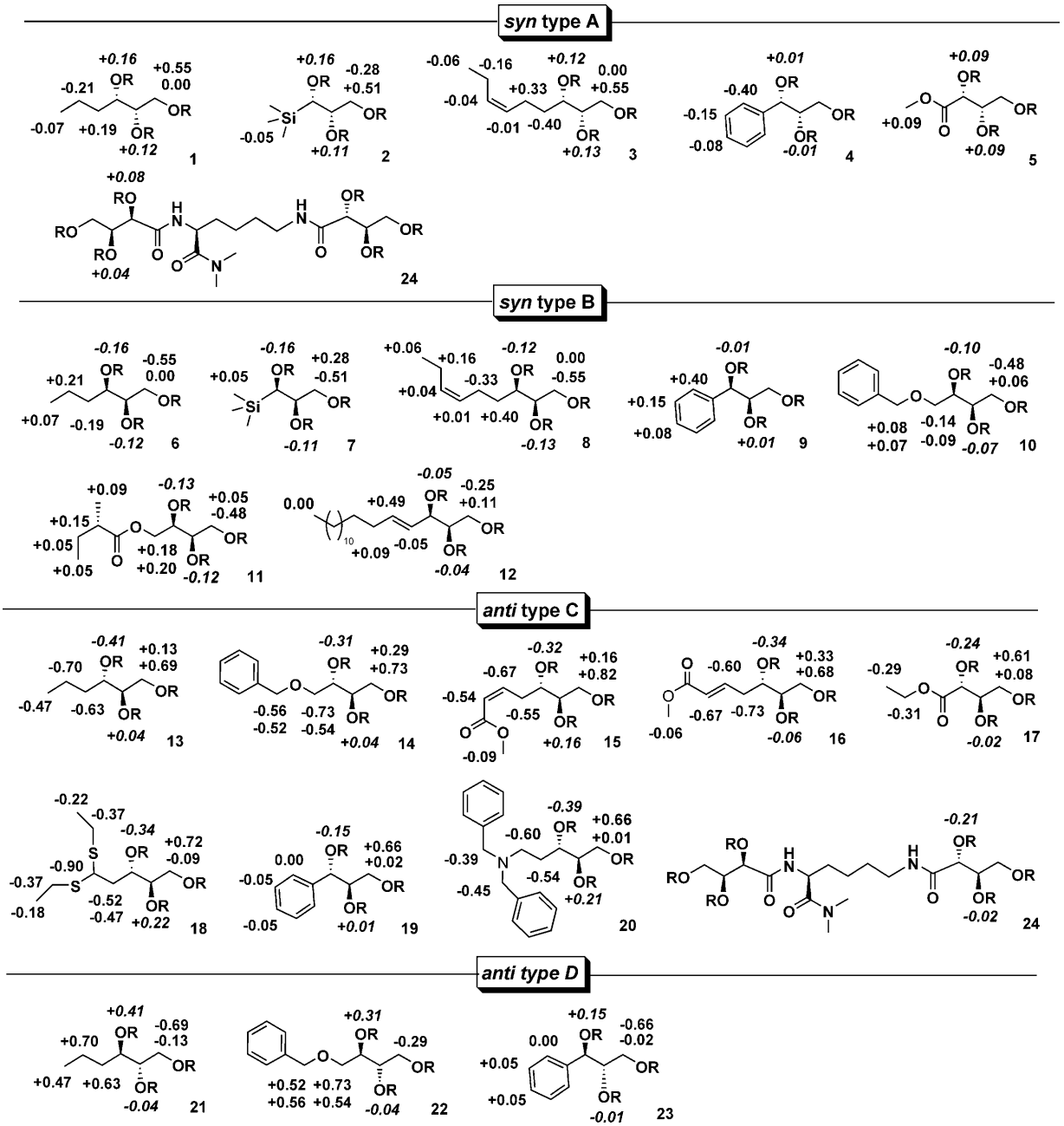

Figure 3. The $\Delta\delta^{RS}$ values for the series of tris-MPA esters of 1,2,3-*prim*,*sec*,*sec*-triols **1**–**24** (the $\Delta\delta^{RS}$ values for H(2′) and H(3′) are underlined and highlighted in italic (R = MPA; MPA = α-methoxy-α-trifluorophenylacetate).

The Cα–CO bond in the MPA derivatives of 1,2,3-*prim*, *sec*,*sec*-triols was also studied by using CD spectroscopy. The tris-MPA esters of (2*S*,3*S*)-hexane-1,2,3-triol (**6**, *syn* type A) and (2*S*,3*R*)-hexane-1,2,3-triol (**13**, *anti* type D) were taken as model substrates (Figure 5). The tris-(*R*)-MPA and tris-(*S*)-MPA esters of the two triols present a negative and positive Cotton effect, respectively ($\Delta\varepsilon = -43.42$ and $+43.81\ cm^2mol^{-1}$ for the *syn* type A triol; $\Delta\varepsilon = -35.02$ and $+39.23\ cm^2mol^{-1}$ for the *anti* type D triol), and these outcomes are associated with the predominance of the *sp* over the *ap* conformer in all cases.[13] In addition, the tris-MPA esters revealed the most intense CD bands, followed by the bis-MPA esters and then the mono-MPA esters, a finding that is consistent with an additive contribution of the *sp* conformer of each MPA auxiliary to the final CD spectra.

The rotation around C(1′)–C(2′) bond: Analysis of vicinal coupling constants and selective deuteration studies: To study the C(1′)–C(2′) bond, it was necessary to combine the information extracted from the vicinal coupling constant values (^3J) with the results of enantioselective deuteration experiments on the methylene protons. With this aim in mind, the four diastereoisomers of hexane-1,2,3-triol were

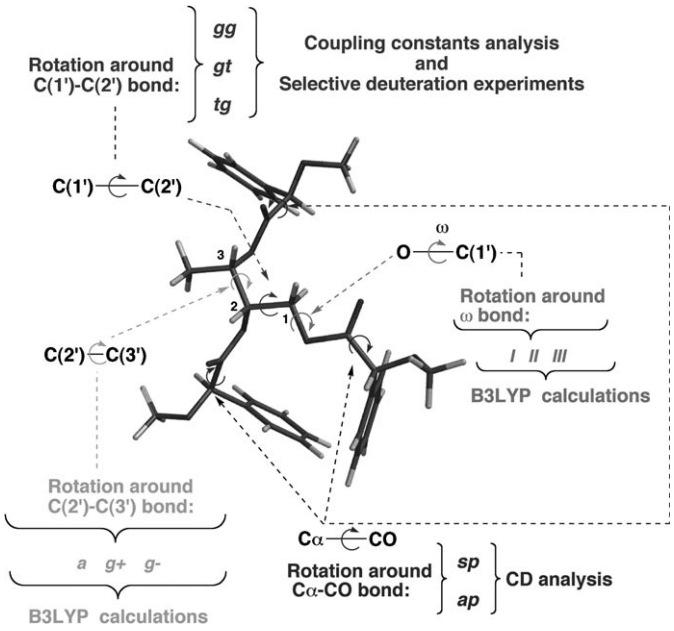

Figure 4. Main conformational processes in the tris-MPA esters of 1,2,3-*prim*,*sec*,*sec*-triols: rotations around the Cα–CO bond (conformers *sp* and *ap*), the O–C(1′) bond (conformers I–III), the C(1′)–C(2′) bond (conformers *gg*, *gt*, and *tg*), and the C(2′)–C(3′) bond (conformers *a*, g^+, and g^-).

Table 1. Vicinal coupling constant values and chemical shifts of the methylene protons of the tris-MPA derivatives of the four diastereoisomers of hexane-1,2,3-triol.

Triol	Derivative[a]	Low-field δ [ppm]	Low-field ^3J [Hz]	High-field δ [ppm]	High-field ^3J [Hz]
syn type A	(*R*)-MPA	3.87	6.7	4.20	3.5
	(*S*)-MPA	3.65	4.5	3.87	7.3
syn type B	(*R*)-MPA	3.65	4.5	3.87	7.3
	(*S*)-MPA	3.87	6.7	4.20	3.5
anti type C	(*R*)-MPA	3.47	8.0	4.20	2.9
	(*S*)-MPA	4.16	5.8	4.33	3.2
anti type D	(*R*)-MPA	4.16	5.8	4.33	3.2
	(*S*)-MPA	3.47	8.0	4.20	2.9

[a] MPA = α-methoxy-α-trifluorophenylacetate.

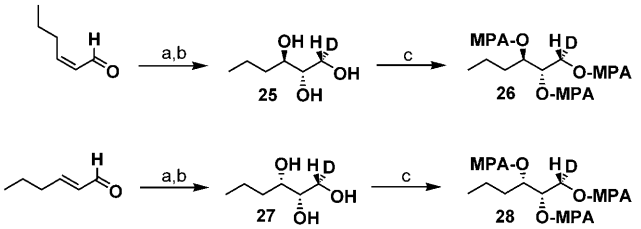

Scheme 1. Preparation of the tris-MPA ester derivatives of $[D_1]$-(1*S*,2*S*,3*R*)-hexane-1,2,3-triol and $[D_1]$-(1*S*,2*S*,3*S*)-hexane-1,2,3-triol. a) Bu_3SnD, (*S*)-Binol, $[Ti(iPrO)_4]$, TFA, 4-Å MS, Et_2O, from −78 to −25 °C; b) ADmixα, *tert*-BuOH/H_2O, RT; c) MPA, EDC, DMAP, CH_2Cl_2, RT. Binol = 1,1′-bi-2-naphthol, DMAP = 4-dimethylaminopyridine, EDC = *N*′-(3-dimethylaminopropyl)-*N*-ethylcarbodiimide, MPA = TFA = trifluoroacetic acid.

derivatized with both enantiomers of MPA and the signals of the methylene protons were analyzed. The values of the ^3J coupling constants for the methylene protons were in the same range in all four cases as those reported for the bis-MPA esters of 1,2-*prim*,*sec*-diols[8c] (i.e., $^3J = 3.5$ and 6.7 Hz), thus suggesting that *gt* and *tg* are the main conformers[14] depending on the configuration of the triol (Table 1).

To determine which conformer, *gt* or *tg*, corresponds to each configuration, the tris-MPA esters of *pro-S* deuterated (1*S*,2*S*,3*R*)-hexane-1,2,3-triol (**26**, *anti* type D) and *pro-S* deuterated (1*S*,2*S*,3*S*)-hexane-1,2,3-triol (**28**, *syn* type A) were prepared (Scheme 1). In this procedure, *cis*- and *trans*-hex-2-enal were enantioselectively reduced with Bu_3SnD in the presence of (*S*)-Binol,[15] followed by the asymmetric dihydroxylation of the double bond with ADmixα,[16] and final esterification of the resulting triols with MPA.

The ^{1}H NMR spectra of the four deuterated *syn* type A and *anti* type D tris-MPA esters (both tris-MPA esters of the two triols) revealed the *pro-S* H atom as the methylene proton with the larger ^3J coupling constant, thus indicating that *tg* is the main conformer around the C(1′)–C(2′) bond in all cases (Figure 6 and Table 1). In the enantiomeric *syn* type B and *anti* type D tris-MPA esters; therefore, the *pro-*

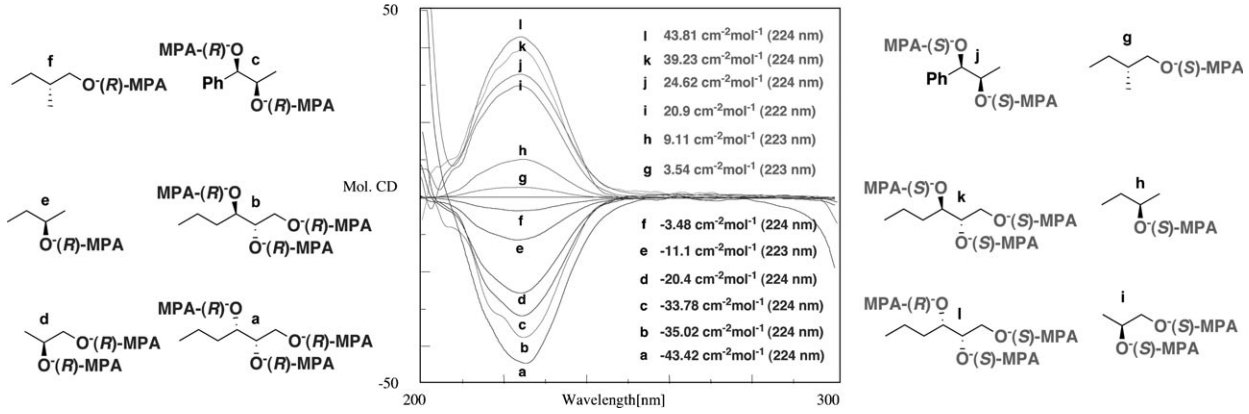

Figure 5. CD spectra of the MPA esters of a chiral primary alcohol (**f** and **g**), a chiral secondary alcohol (**e** and **h**), a chiral 1,2-*sec*,*sec*-diol (**c** and **j**), a chiral 1,2-*prim*,*sec*-diol (**d** and **i**), and two chiral 1,2,3-*prim*,*sec*,*sec*-triols (**a**, **b**, **k**, and **l**) ($c = 1 \times 10^{-5}$ M in MeOH).

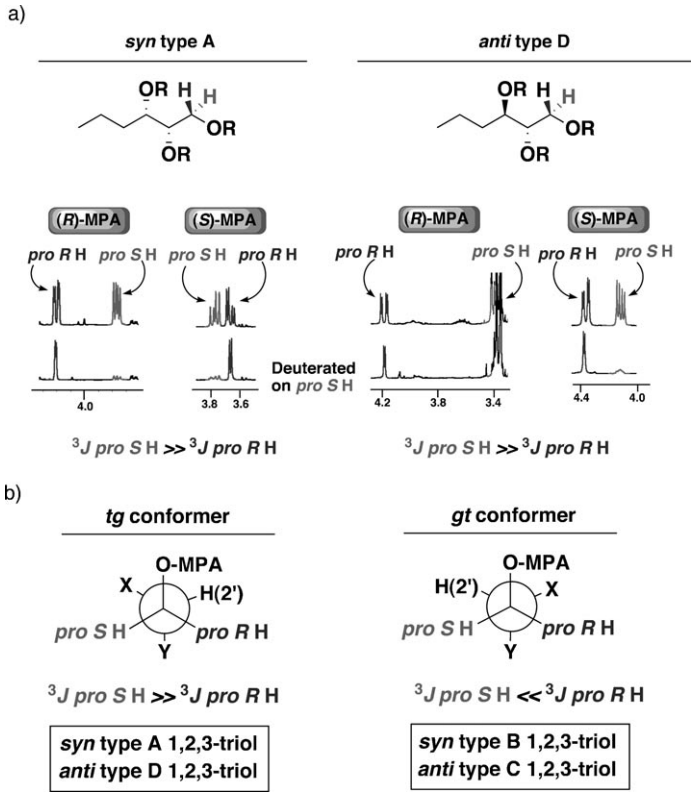

Figure 6. a) Partial ^{1}H NMR spectra that shows the methylene protons of the tris-MPA esters of (2*S*,3*S*)-hexane-1,2,3-triol (*syn* type A), (2*S*,3*R*)-hexane-1,2,3-triol (*anti* type D), and *pro*-*S* deuterated analogues. b) Main conformation around C(1′)−C(2′) bond in the tris-MPA esters of 1,2,3-*prim*,*sec*,*sec*-triols.

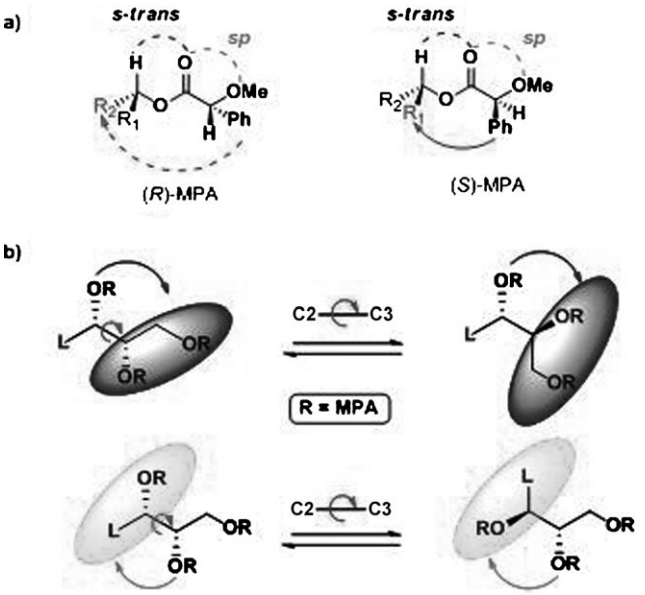

Figure 7. a) The *s*-*trans* conformation and selective aromatic shielding effects induced by the MPA auxiliary in this conformation. b) Variation of the shielding caused by the two MPA auxiliaries at the chiral hydroxy groups by rotation around the C(2′)−C(3′) bond in the (*R*)-MPA derivative of *syn* type A 1,2,3-*prim*,*sec*,*sec*-triols.

R H atom is the methylene proton with the larger ^{3}J coupling constant, thus corresponding to *gt* as the main conformer in these derivatives.

The rotation around the C(2′)−C(3′) bond: a practical study: Previous studies carried out on the MPA esters of secondary alcohols, primary/secondary, and secondary/secondary 1,2-diols showed that the carbonyl group of the MPA auxiliaries linked to the secondary hydroxy groups are oriented in the same plane as CHα to give an *s*-*trans* conformation[8a–d,12] (Figure 7 a). In the case of the tris-MPA esters, as the MPA auxiliaries are oriented in an *sp* conformation, the aromatic shielding effects caused by the two MPA auxiliaries in the esterified secondary hydroxy groups could be predicted provided that the rotation around the C(2′)−C(3′) bond does not modify the shielding pattern associated with these auxiliaries.

The finding that the anisotropic contributions of the MPA auxiliaries linked to the chiral hydroxy groups do not vary with rotation around the C(2′)−C(3′) bond is graphically illustrated in Figure 7 for the tris-(*R*)-MPA derivative of the *syn* type A configuration. If these auxiliaries shield a substituent at either the right- or left-hand side of the chiral center, this substituent remains under the anisotropic effects of the same MPA auxiliary whether rotation around the C(2′)−C(3′) bound occurs or not. Although this fact is independent of the absolute stereochemistries of the auxiliary and triol, the most relevant conformers around this bond were taken into account when performing theoretical energy calculations to optimize the minimum energy structures.

The preference around the O−C(1′) bond: structure optimization and energy calculations: The rotational equilibrium around the O−C(1′) bond was studied by performing DFT (B3LYP) calculations[17] on the tris-MPA esters of (2*S*,3*S*)-butane-1,2,3-triol (*syn* type A) and (2*R*,3*S*)-butane-1,2,3-triol (*anti* type C) as model structures. All starting entries incorporated the *sp* conformer (for the Cα−CO bond) and *tg* or *gt* conformers (for the C(1′)−C(2′) bond), as deduced experimentally. The most relevant conformers analyzed around the O−C(1′) bond were: 1) conformer I, with the carbonyl group of the MPA auxiliary at C(1′) bisecting the angle formed by the two methylene protons; 2) conformer II, with the carbonyl group of the MPA auxiliary at C(1′) coplanar to the *pro*-*S* H atom; and 3) conformer III, with the carbonyl group of the MPA auxiliary at C(1′) coplanar to the *pro*-*R* H atom. Additionally, the most representative conformers involved in the rotation around C(2′)−C(3′) bond were analyzed: conformers *a*, *g*+, and *g*−, with the two MPA esters at 180, 60, and −60°, respectively.

The results of the structure and energy calculations were in full agreement with the *sp* (Cα−CO bond), *gt* and *tg* (C(1′)−C(2′) bond), and *s*-*trans* (C=O−CHα) conformations, as these resulted from the calculated structures of lower energy (see Table S1 in the Supporting Information). The

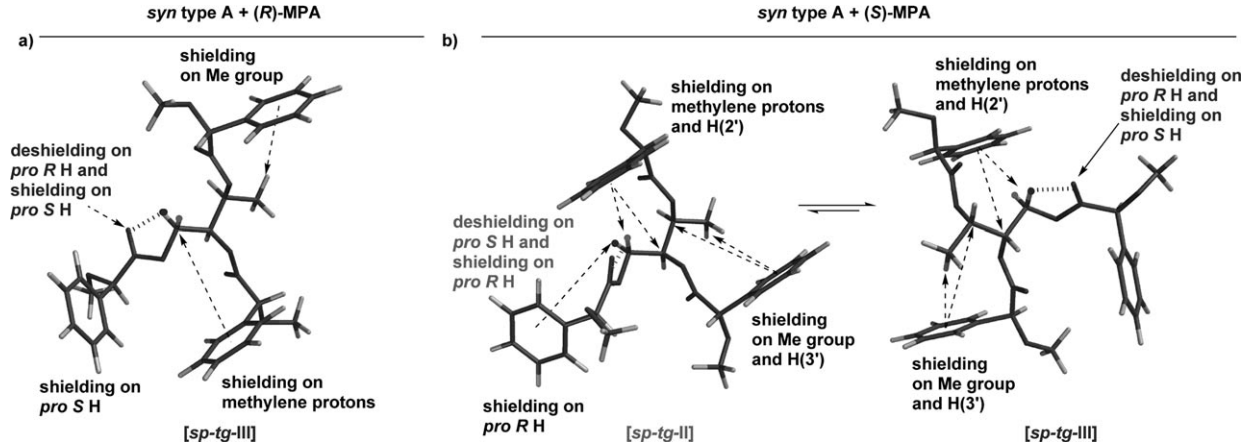

Figure 8. Representative conformers of the *syn* type A a) tris-(*R*)-MPA and b) tris-(*S*)-MPA ester of butane-1,2,3-triol.

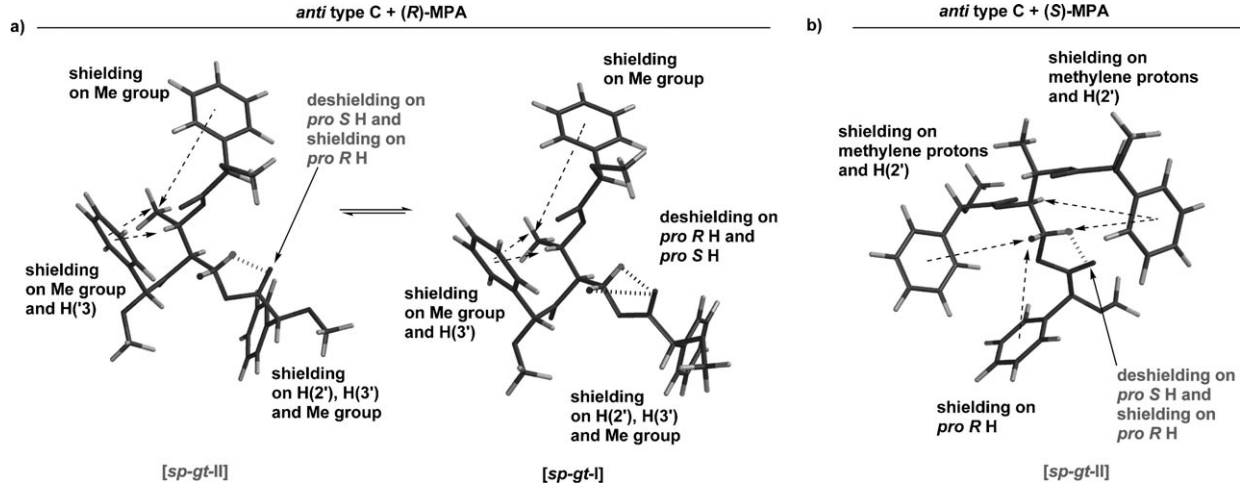

Figure 9. Representative conformers of the *anti* type C a) tris-(*R*)-MPA and b) tris-(*S*)-MPA ester of butane-1,2,3-triol.

complete anisotropic effects associated with the most stable conformations are graphically depicted in Figures 8 and 9 (for the *syn* and *anti* configurations, respectively). The results can be summarized as follows:

1) *syn* type A tris-(*R*)-MPA ester: the most stable conformer is [*sp-tg*-III].
2) *syn* type A tris-(*S*)-MPA ester: there is an equilibrium between the [*sp-tg*-II] and [*sp-tg*-III] conformers.
3) *syn* type B tris-(*R*)-MPA ester: there is an equilibrium formed by the [*sp-gt*-III] and [*sp-gt*-II] conformers, which are the enantiomers of those found for the *syn* type A tris-(*S*)-MPA ester derivative.
4) *syn* type B tris-(*S*)-MPA ester: the most stable conformer is [*sp-gt*-II], which is the enantiomer of the conformer found for the *syn* type A tris-(*R*)-MPA ester derivative.
5) *anti* type C tris-(*R*)-MPA ester: there is an equilibrium between the [*sp-gt*-I] and [*sp-gt*-II] conformers.
6) *anti* type C tris-(*S*)-MPA ester: the most stable conformer is [*sp-gt*-II].
7) *anti* type D tris-(*R*)-MPA ester: the most stable conformer is [*sp-tg*-III], which is the enantiomer of the conformer found for the *syn* type A tris-(*R*)-MPA ester derivative.
8) *anti* type D tris-(*S*)-MPA ester: the conformational equilibrium is formed by the [*sp-tg*-I] and [*sp-tg*-III] conformers, which are enantiomers of the conformers found for the *anti* type C tris-(*S*)-MPA ester derivative.

Low-temperature NMR spectroscopic studies: The last step in the conformational analysis of the tris-MPA esters of 1,2,3-*prim*,*sec*,*sec*-triols involved validating the conformations previously deduced by dynamic NMR spectroscopic experiments. A drop in temperature would be expected to give an increase in the relative population of the most stable conformers and a decrease in the relative population of the less stable conformers. In this way, the shielding effects associated with the major conformations will be increased and those of the minor conformations will be decreased. Conse-

quently, all of these changes will be reflected in the NMR spectra.[18] Experimental evidence to identify such conformers was obtained from low-temperature ^{1}H NMR spectroscopic experiments carried out on the tris-MPA esters of (2*S*,3*S*)-hexane-1,2,3-triol (**1**, *syn* type A) and the tris-MPA esters of (2*R*,3*S*)-hexane-1,2,3-triol (**13**, *anti* type C).

A comparison of the ^{1}H NMR spectra of the *syn* type A tris-(*R*)-MPA ester of hexane-1,2,3-triol ((*R*)-**1**) recorded at different temperatures (Figure 10a) revealed the following:

1) The methylene proton signals move in opposite directions at lower temperature: The signals for the *pro-S* H and *pro-R* H atoms shift upfield and downfield, respectively. These movements are in full agreement with a relative population increase of the [*sp-tg*-III] conformer, in which the *pro-R* H atom is deshielded by the carbonyl group of the MPA unit at C(1′) and shielded by the aromatic ring of the MPA unit at C(2′), whereas the *pro-S* H atom is shielded by the carbonyl and aryl groups of the MPA unit at C(1′) and by the aromatic ring of the MPA unit at C(2′) (Figure 8a).
2) The signals for H(2′) and H(3′) move to lower field when the temperature is decreased. The transfer of population from the less stable *ap* rotamer to the more stable *sp* rotamer of the MPA units at C(2′) and C(3′) results in an overall decrease of the shielding effects that act on these protons (Figure 8a).
3) The signals for the propyl protons move upfield at lower temperatures. This change is due to the larger shielding effects induced by the phenyl ring of the MPA unit at C(3′) as a result of the relative population increase of the *sp* conformer (Figure 8a).

Clearly, this behavior must be the same as that expected for the tris-(*S*)-MPA ester of the corresponding *syn* type B triol by simply changing the *pro-R* H atom for the *pro-S* H atom, and vice versa, and the [*sp-tg*-III] conformer for the [*sp-gt*-II] conformer.

A comparison of the NMR spectra of the *syn* type A tris-(*S*)-MPA ester of hexane-1,2,3-triol ((*S*)-**1**) recorded at different temperatures (Figure 10b) revealed the following:

1) The signals for the methylene proton move to higher field when the temperature drops. These shifts can be explained considering the relative population increases of the [*sp-tg*-II] and [*sp-tg*-III] conformations. In these conformations, the *pro-R* H atom is shielded by the phenyl rings of the MPA units at C(1′) and C(3′) and the *pro-S* H atom by the phenyl ring of the MPA unit at C(3′). In addition, the opposite anisotropic effects due to the carbonyl group of the MPA unit at C(1′) in each conformer are mostly cancelled out (Figure 8b).
2) The H(2′) and H(3′) signals shift upfield as the temperature decreases. Both protons experience greater aromatic shielding effects by the MPA units at C(2′) and C(3′) due to the relative population increase of the *sp* conformer (Figure 8b).
3) The signals for the propyl protons shift upfield at lower temperatures. These shifts are caused by the larger aromatic shielding effect produced by the phenyl ring of the MPA unit at C(2′) due to the higher populations of the *sp* conformer (Figure 8b).

Once again, this behavior must clearly be equal to that expected for the tris-(*R*)-MPA ester of the corresponding

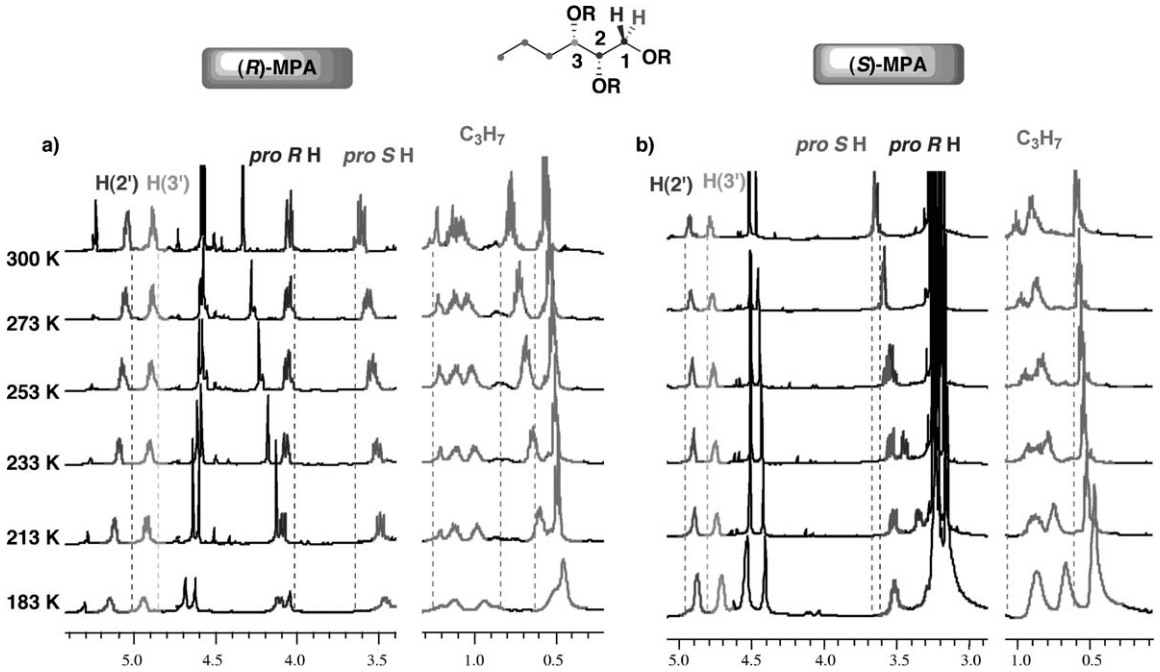

Figure 10. Partial ^{1}H NMR spectra of the a) tris-(*R*)-MPA and b) tris-(*S*)-MPA esters of (2*S*,3*S*)-hexane-1,2,3-triol recorded at different temperatures (300–183 K).

syn type B triol by simply changing the *pro-R* H atom for the *pro-S* H atom, and vice versa, and the [*sp-tg*-II] and [*sp-tg*-III] conformers for the [*sp-gt*-III] and [*sp-gt*-II] conformers, respectively.

A comparison of the NMR spectra of the *anti* type C tris-(*R*)-MPA ester of hexane-1,2,3-triol ((*R*)-**13**) recorded at different temperatures (Figure 11a) revealed the following:

1) The signals for the methylene protons remain almost unchanged on decreasing the temperature and shift significantly only at the lowest end of the temperature range. This observation points to an equilibrium between the [*sp-gt*-I] and [*sp-gt*-II] conformers[19] (Figure 9a). At very low temperatures, a relative population increase of the [*sp-gt*-I] conformer is observed (both methylene protons resonate at closer chemical shifts).[20]
2) The signal for H(2′) remains almost unchanged and the H(3′) signal is shifted to higher field as the temperature decreases. In the case of H(2′), the increase in the aromatic shielding effects produced by the MPA unit at C(1′) is counteracted by the decrease in the aromatic shielding effects produced by the MPA units at C(2′) and C(3′) due to the population transfer from the less stable *ap* rotamer to the more stable *sp* rotamer. For its part, H(3′) experiences higher aromatic shielding effects by the MPA units at C(1′) and C(2′) due to the larger populations of the *sp* conformer (Figure 9a).
3) The signals for the propyl protons are shifted upfield at lower temperatures. This change is promoted by the increase in the aromatic shielding effects produced by the phenyl rings of the MPA units at C(2′) and C(3′), which are caused by the relative population increase of the *sp* conformer (Figure 9a).

Once again, it is clear that this behavior must be equal to that expected for the tris-(*S*)-MPA ester of the corresponding *anti* type D triol by simply changing the *pro-R* H atom for the *pro-S* H atom, and vice versa, and the [*sp-gt*-I] and [*sp-gt*-II] conformers for the [*sp-tg*-I] and [*sp-tg*-III] conformers, respectively.

A comparison of the NMR spectra of the *anti* type C tris-(*S*)-MPA ester of hexane-1,2,3-triol ((*S*)-**13**) recorded at different temperatures (Figure 11b) revealed the following:

1) The methylene protons behave differently on lowering the temperature: the signal for the *pro-S* H atom is markedly shifted to higher field, whereas the signal for the *pro-R* H atom remains almost unchanged. This observation can be explained in terms of the relative population increase of the [*sp-gt*-II] conformer, in which the *pro-R* H atom is deshielded by the carbonyl group of the MPA unit at C(1′) and shielded by the aromatic rings of the MPA units at C(2′) and C(3′) and the *pro-S* H atom is shielded by the carbonyl group and the aromatic ring of the MPA at C(1′) and by the aromatic rings of the MPA units at C(2′) and C(3′) (Figure 9b).
2) The H(2′) signal is shifted upfield and the H(3′) signal is shifted downfield at lower temperatures. Proton H(2′) experiences a higher aromatic shielding effect induced by the MPA unit at C(3′) due to the relative population increase of the *sp* conformer, whereas H(3′) experiences lower aromatic shielding effects induced by the MPA

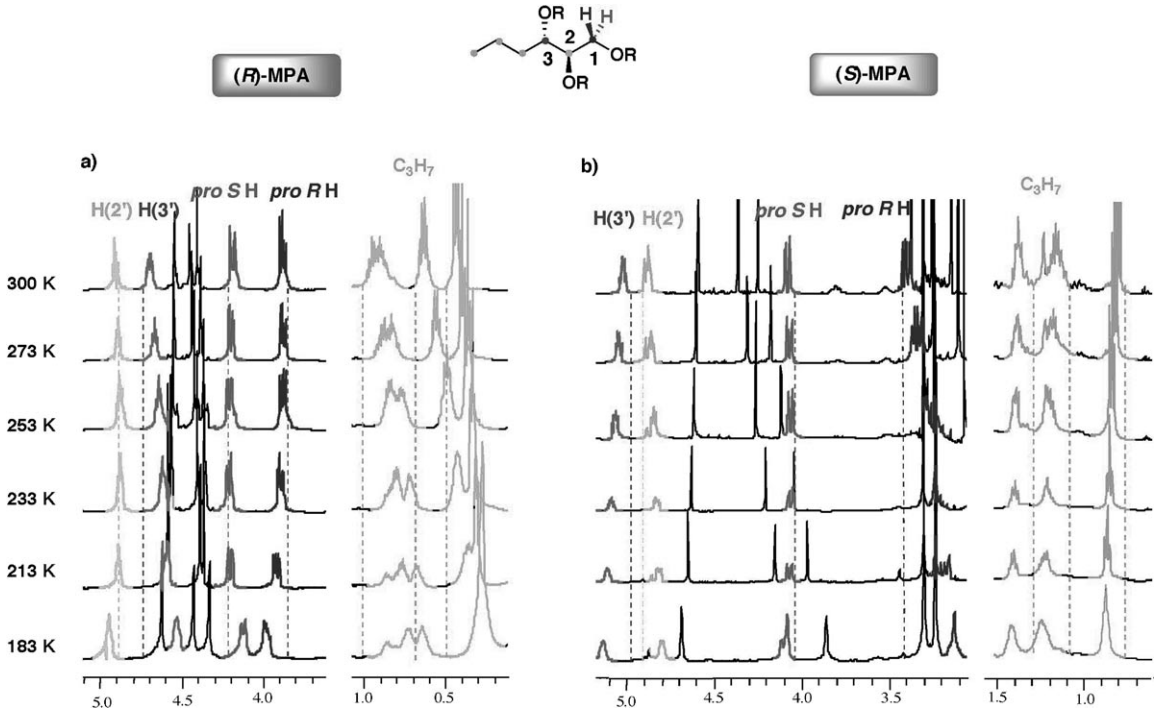

Figure 11. Partial ^{1}H NMR spectra of the a) tris-(*R*)-MPA and b) tris-(*S*)-MPA esters of (2*R*,3*S*)-hexane-1,2,3-triol recorded at different temperatures (300–183 K).

unit at C(2′) due to the population transfer from the *ap* rotamer to the *sp* rotamer (Figure 9b).
3) The signals for the propyl protons move to lower field at lower temperatures. The population decrease of the *ap* rotamer in favor of the *sp* rotamer of the MPA units at C(2′) and C(3′) causes the downfield shift of these signals (Figure 9b).

This behavior must clearly be equal to that expected for the tris-(*R*)-MPA ester of the corresponding *anti* type D triol by changing the *pro-R* H atom for the *pro-S* H atom, and vice versa, and the [*sp-gt*-II] conformer for the [*sp-tg*-III] conformer.

From these low-temperature NMR spectroscopic experiments, it can be concluded that the majority of the NMR-significant conformations concur with those previously deduced from the conformational analyses and energy calculations.

The correlation between the NMR spectra and the absolute configuration: Once the NMR-representative conformers of the tris-MPA esters of 1,2,3-*prim*,*sec*,*sec*-triols have been determined (Figures 8 and 9), it is possible to predict the signs and intensities of the $\Delta\delta^{RS}$ values for H(2′) and H(3′) and to ascertain whether there is a correlation between these values and the absolute stereochemistry of the substrate. Thus:

1) *syn* type A: H(2′) and H(3′) are more shielded in the tris-(*S*)-MPA system than in the tris-(*R*)-MPA derivative; therefore, a positive $\Delta\delta^{RS}$ value should be expected for these protons.
2) *syn* type B: H(2′) and H(3′) are more shielded in the tris-(*R*)-MPA system than in the tris-(*S*)-MPA derivative; therefore, a negative $\Delta\delta^{RS}$ value should be expected for these protons.
3) *anti* type C: H(3′) is more shielded in the tris-(*R*)-MPA system than in the tris-(*S*)-MPA derivative; therefore, a negative $\Delta\delta^{RS}$ value should be expected for H(3′). For its part, H(2′) is under comparable shielding effects in both derivatives, thus making it impossible to predict the sign of the $\Delta\delta^{RS}$ value in this case.
4) *anti* type D: H(3′) is more shielded in the tris-(*S*)-MPA system than in the tris-(*R*)-MPA derivative; therefore, a positive $\Delta\delta^{RS}$ value should be expected for H(3′). For its part, H(2′) is under comparable shielding effects in both derivatives, thus making it impossible to predict the sign of the $\Delta\delta^{RS}$ value in this case.

Overall, points (1)—(4) indicate that the $\Delta\delta^{RS}$ value of H(3′) should be positive in *syn* type A and *anti* type D triols, but negative in *syn* type B and *anti* type C triols.

Bearing in mind the relative intensities of the anisotropic effects acting on H(2′) and H(3′), the following facts are found:

In *syn* triols, the overall contribution of each auxiliary is very similar for both H(2′) and H(3′). Namely:

1) *syn* type A: H(2′) and H(3′) are shielded by two auxiliaries in the tris-(*R*)-MPA derivative, whereas these two protons are not shielded by any auxiliary in the tris-(*S*)-MPA derivative. As a result, the $\Delta\delta^{RS}$ values of H(2′) and H(3′) should have identical signs and be of similar intensities; thus, the absolute value of the difference between them should be close to zero (expressed as $|\Delta(\Delta\delta^{RS})| \approx 0$).
2) *syn* type B: H(2′) and H(3′) are not shielded by any auxiliary in the tris-(*R*)-MPA derivative, whereas both are shielded by two auxiliaries in the tris-(*S*)-MPA derivative. Therefore, the $\Delta\delta^{RS}$ values of H(2′) and H(3′) should have identical signs and be of similar intensities; thus, the absolute value of the difference between them should be close to zero (i.e., $|\Delta(\Delta\delta^{RS})| \approx 0$).

In *anti* triols, the overall contribution of each auxiliary is quite different for H(2′) and H(3′). Namely:

3) *anti* type C: H(2′) is shielded by one auxiliary in both tris-(*R*)- and tris-(*S*)-MPA derivatives; thus, intensities close to zero are expected for the $\Delta\delta^{RS}$ value of H(2′). In contrast, H(3′) is heavily shielded in the tris-(*R*)-MPA derivative by two auxiliaries, but is not shielded by any auxiliary in the tris-(*S*)-MPA derivative, with a large $\Delta\delta^{RS}$ value predicted for this proton. Therefore, values of $|\Delta(\Delta\delta^{RS})|$ that are clearly higher than zero are expected ($|\Delta(\Delta\delta^{RS})| \gg 0$).
4) *anti* type D: H(2′) is shielded by one auxiliary in both tris-(*R*)-MPA and tris-(*S*)-MPA derivatives; thus, intensities close to zero are expected for the $\Delta\delta^{RS}$ value of H(2′). In contrast, H(3′) is heavily shielded in the tris-(*S*)-MPA derivative by two auxiliaries, but is not shielded by any auxiliary in the tris-(*R*)-MPA derivative with a large $\Delta\delta^{RS}$ value predicted for H(3′). Therefore, $|\Delta(\Delta\delta^{RS})|$ values that are clearly higher than zero are expected ($|\Delta(\Delta\delta^{RS})| \gg 0$).

In summary, the $\Delta\delta^{RS}$ value of H(3′) could be used to distinguish between the pairs *syn* type A/*anti* type D (being positive) and *syn* type B/*anti* type C (being negative). The $|\Delta(\Delta\delta^{RS})|$ parameter could be used to distinguish between the pairs *syn* type A/*syn* type B ($|\Delta(\Delta\delta^{RS})| \approx 0$) and *anti* type C/*anti* type D ($|\Delta(\Delta\delta^{RS})| \gg 0$). So, by using these two parameters together, it must be possible to assign the absolute stereochemistry of a triol of unknown configuration, as depicted in Figure 12.

The validity of these predictions[21] and the possible use of the $\Delta\delta^{RS}$ value of H(3′) and $|\Delta(\Delta\delta^{RS})|$ as diagnostic parameters were previously confirmed with compounds **1**–**24** (Figure 3). In this respect, compounds **1**–**5** (*syn* type A) and **6**–**12** (*syn* type B) showed positive and negative values for the $\Delta\delta^{RS}$ value of H(3′), respectively. In addition, the values of $|\Delta(\Delta\delta^{RS})|$ in both sets of compounds were in the range $\Delta\delta = 0.00$–0.06 ppm. Compounds **13**–**20** (*anti* type C) and **21**–**23** (*anti* type D) showed negative and positive $\Delta\delta^{RS}$ values for H(3′), respectively. In these examples, the $|\Delta$-

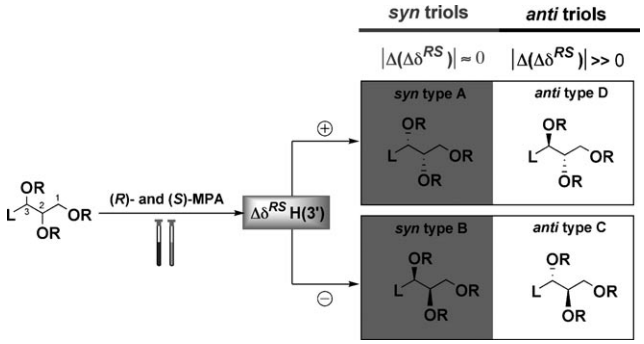

Figure 12. Graphical model to assign the absolute configuration of 1,2,3-*prim*,*sec*,*sec*-triols.

$(\Delta\delta^{RS})|$ values were in the range $\Delta\delta = 0.16$–0.53 ppm, that is, significantly different from those obtained for the *syn* configuration. The hexakis-ester **24**, bearing both *syn* type A and *anti* type C tris-esters, warrants particular attention as both triol moieties presented $\Delta\delta^{RS}$ values for H(3′) and $|\Delta(\Delta\delta^{RS})|$ parameters according to their absolute stereochemistry.

It is also worth pointing out that although the behavior of the $\Delta\delta^{RS}$ values of H(3′) and $|\Delta(\Delta\delta^{RS})|$ parameters in (1*S*,2*S*)-1-phenylpropane-1,2,3-triol (**4**; *syn* type A) and (1*R*,2*R*)-1-phenylpropane-1,2,3-triol (**9**; *syn* type B) fit with their stereochemistries, both showed $\Delta\delta^{RS}$ values for H(3′) and H(2′) that were close to the experimental error.[22] The analogous compounds (1*S*,2*R*)-1-phenylpropane-1,2,3-triol (**19**; *anti* type C) and (1*R*,2*S*)-1-phenylpropane-1,2,3-triol (**20**; *anti* type D), also in keeping with their stereochemistries, showed $\Delta\delta^{RS}$ values for H(2′) that were close to the experimental error along with the lowest $|\Delta(\Delta\delta^{RS})|$ values of any of the *anti* triols tested. All of these findings suggest that the anisotropic effect due to the extra aromatic ring is added to the expected effect, and this fact must be taken into account when dealing with similar substrates.

Finally, theoretical NMR spectroscopic calculations (GIAO)[17,23] were performed (see Table S2 in the Supporting Information). The chemical shifts were obtained from the conformations of lowest energy previously calculated for the *syn* type A and *anti* type C tris-MPA esters of butane-1,2,3-triol. In this way, a positive $\Delta\delta^{RS}$ value of H(3′) ($\Delta\delta = +0.22$ ppm) along with a small $|\Delta(\Delta\delta^{RS})|$ parameter ($\Delta\delta = 0.04$ ppm) for the *syn* type A triol and a negative $\Delta\delta^{RS}$ value of H(3′) ($\Delta\delta = -0.68$ ppm) along with a large $|\Delta(\Delta\delta^{RS})|$ parameter ($\Delta\delta = 1.44$ ppm) for the *anti* type C triol were calculated. These theoretical data match very well with the $\Delta\delta^{RS}$ value of H(3′) and the $|\Delta(\Delta\delta^{RS})|$ patterns expected for these configurations.

In the case of the proton signals of the substituent directly attached to C(3′) (i.e., the propyl groups in **1**, **6**, **13**, and **21** in Figure 3; generally represented as group L), both theoretical and experimental studies reveal that the signs of their $\Delta\delta^{RS}$ values can be predicted for *anti* triols (Figure 9). In addition, the opposite signs of the $\Delta\delta^{RS}$ values for these protons result from the combination of anisotropic effects of both MPA derivatives: negative values are obtained for *anti* type C triols (i.e., **13**) and positive values for *anti* type D triols (i.e., **21**). Therefore, the signs of the $\Delta\delta^{RS}$ values for the L groups in *anti* triols can be correlated with their absolute stereochemistry (Figure 3).

On the contrary, no general pattern can be inferred for *syn* triols (Figures 3 and 8), and consequently, in these cases the signs of the $\Delta\delta^{RS}$ values for the L groups are not diagnostic.

The identification of *pro-R* and *pro-S* methylene protons: Methylene protons are under the influence of a complex combination of anisotropic effects that make it unfeasible to predict their $\Delta\delta^{RS}$ values. Nevertheless, a definite type of behavior was observed in the tris-MPA derivatives of each diastereoisomer of hexane-1,2,3-triol (see Figure 13 and Table 2). A description of these behaviors is outlined below:

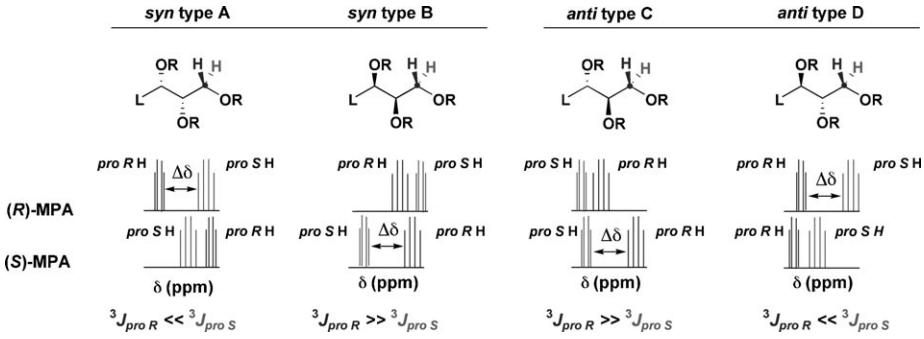

Figure 13. Graphical representation of the behavior found for the methylene protons in the tris-MPA esters of 1,2,3-*prim*,*sec*,*sec*-triols.

1) *syn* type A: The two methylene protons resonate further from each other in the tris-(*R*)-MPA than in the tris-(*S*)-MPA derivative. Moreover, in the tris-(*R*)-MPA derivative the *pro-S* H atom (larger ^3J coupling constant) resonates at higher field than the *pro-R* H atom (smaller ^3J coupling constant). The opposite holds for the tris-(*S*)-MPA derivative, in which the *pro-S* H atom (larger ^3J coupling constant) resonates at lower field and the *pro-R* H atom (smaller ^3J coupling constant) at higher field.
2) *syn* type B: The two methylene protons resonate closer to each other in the tris-(*R*)-MPA than in the tris-(*S*)-MPA derivative. Moreover, in the tris-(*R*)-MPA derivative the *pro-R* H atom (larger ^3J coupling constant) resonates at lower field than the *pro-S* H atom (smaller ^3J

Table 2. Values of chemical shifts and vicinal coupling constants of the methylene protons in the tris-MPA derivatives of 1,2,3-*prim*,*sec*,*sec*-triols (**1**–**23**).

			Low-field		High-field		
Triol	Type	MPA	δ [ppm]	^3J [Hz]	δ [ppm]	^3J [Hz]	$\lvert\Delta\delta\rvert$ [ppm]
1	A	(*R*)	4.20	3.5	3.77	6.7	0.43
		(*S*)	3.77	7.3	3.65	4.5	0.12
2	A	(*R*)	4.21	4.5	3.59	6.9	0.62
		(*S*)	3.87	6.7	3.70	5.3	0.17
3	A	(*R*)	4.25	3.6	3.77	6.8	0.48
		(*S*)	3.77	7.5	3.70	4.4	0.07
4	A	(*R*)	3.98	3.0	3.39	4.9	0.59
		(*S*)	3.94	3.8	3.63	5.8	0.31
5	A	(*R*)	4.18	5.8	3.83	7.1	0.35
		(*S*)	3.95	6.6	3.50	6.6	0.45
6	B	(*R*)	3.77	7.3	3.65	4.5	0.12
		(*S*)	4.20	3.5	3.77	6.7	0.43
7	B	(*R*)	3.87	6.7	3.70	5.3	0.17
		(*S*)	4.21	4.5	3.59	6.9	0.62
8	B	(*R*)	3.77	7.5	3.70	4.4	0.07
		(*S*)	4.25	3.6	3.77	6.8	0.48
9	B	(*R*)	3.94	3.8	3.63	5.8	0.31
		(*S*)	3.98	3.0	3.39	4.9	0.59
10	B	(*R*)	3.83	6.8	3.68	4.6	0.15
		(*S*)	4.16	3.6	3.77	5.8	0.39
11	B	(*R*)	3.75	6.4	3.68	4.8	0.07
		(*S*)	4.16	3.9	3.70	6.2	0.46
12	B	(*R*)	3.84	5.6	3.84	5.6	0.00
		(*S*)	4.09	3.0	3.73	5.4	0.36
13	C	(*R*)	4.33	3.2	4.06	5.8	0.27
		(*S*)	4.20	2.9	3.37	8.0	0.83
14	C	(*R*)	4.50	2.7	4.10	4.8	0.40
		(*S*)	4.21	2.3	3.35	6.3	0.86
15	C	(*R*)	4.34	3.5	4.17	6.2	0.17
		(*S*)	4.18	3.1	3.35	7.0	0.83
16	C	(*R*)	4.42	3.5	4.02	5.1	0.40
		(*S*)	4.09	3.2	3.34	6.2	0.75
17	C	(*R*)	4.33	5.6	4.33	5.6	0.00
		(*S*)	4.23	5.1	3.70	7.5	0.53
18	C	(*R*)	4.26	3.7	4.14	6.2	0.12
		(*S*)	4.17	3.1	3.42	7.8	0.75
19	C	(*R*)	4.27	3.5	4.12	5.8	0.15
		(*S*)	4.05	3.2	3.46	4.4	0.59
20	C	(*R*)	4.09	3.3	3.93	6.1	0.16
		(*S*)	4.08	3.0	3.27	6.3	0.81
21	D	(*R*)	4.20	2.9	3.37	8.0	0.83
		(*S*)	4.33	3.2	4.06	5.8	0.27
22	D	(*R*)	4.21	2.3	3.35	6.3	0.86
		(*S*)	4.50	2.7	4.10	4.8	0.40
23	D	(*R*)	4.05	3.2	3.46	4.4	0.59
		(*S*)	4.27	3.5	4.12	5.8	0.15

coupling constant). The opposite holds for the tris-(*S*)-MPA derivative, in which the *pro-R* H atom (larger ^3J coupling constant) resonates at higher field and the *pro-S* H atom (smaller ^3J coupling constant) at lower field.

3) *anti* type C: The two methylene protons resonate closer to each other in the tris-(*R*)-MPA than in the tris-(*S*)-MPA derivative. Moreover, in the tris-(*R*)-MPA derivative the *pro-R* H atom (larger ^3J coupling constant) resonates at higher field than the *pro-S* H atom (smaller ^3J coupling constant). The same holds for the tris-(*S*)-MPA derivative, in which the *pro-R* H atom (larger ^3J coupling constant) resonates at higher field and the *pro-S* H atom (smaller ^3J coupling constant) at lower field.
4) *anti* type D: The two methylene protons resonate further from each other in the tris-(*R*)-MPA than in the tris-(*S*)-MPA derivative. Moreover, in the tris-(*R*)-MPA derivative the *pro-S* H atom (larger ^3J coupling constant) resonates at higher field than the *pro-R* H atom (smaller ^3J coupling constant). The same holds for the tris-(*S*)-MPA derivative, in which the *pro-S* H atom (larger ^3J coupling constant) resonates at higher field and the *pro-R* H atom (smaller ^3J coupling constant) at lower field.

It must be noted that although **1**–**3**, **6**–**8**, **10**, **11**, **13**–**16**, and **18**–**23** showed the same behavior related to the methylene protons as the tris-MPA esters of hexane-1,2,3-triol (Table 2), some inconsistencies were found[24] (i.e., **4**, **5**, **9**, **12**, and **17** in Table 2). Thus, in enantiomeric compounds **4** (*syn* type A) and **9** (*syn* type B), the methylene protons showed an inversion of the expected values for the ^3J coupling constant in their tris-(*S*)-MPA and tris-(*R*)-MPA derivatives, respectively (the methylene proton with the larger ^3J coupling constant resonated at lower field than the other proton for **4** and the opposite held for **9**). In **12** (*syn* type B) and **17** (*anti* type C), the methylene protons showed the same values for the ^3J coupling constant in their tris-(*S*)-MPA derivatives. Finally, for **5** (*syn* type A) both methylene protons showed the same ^3J coupling constant in the tris-(*S*)-MPA derivative and the opposite relative chemical shifts to those expected (i.e., the methylene protons resonate at closer chemical shifts in the tris-(*R*)-MPA than in the tris-(*S*)-MPA derivative). These inconsistencies are presumably related to the complexity of the anisotropic effects that act on the methylene protons, which are very sensitive to changes in the conformational equilibria of the C(1′)–C(2′) and O–C(1′) bonds. For this reason, only after the absolute configuration has been determined can the behavior of the methylene protons be compared with that depicted in Figure 13 to identify the *pro-R* and *pro-S* protons.

Conclusions

The conformational compositions of tris-MPA ester derivatives of 1,2,3-*prim*,*sec*,*sec*-triols have been determined by using theoretical and experimental data (energy and chemical-shift calculations along with CD and NMR spectroscopic experiments). A detailed study of the overall anisotropic effects that act on H(2′) and H(3′) has revealed the correlation between the absolute configuration of the substrate and the $\Delta\delta^{RS}$ value of H(3′) and $|\Delta(\Delta\delta^{RS})|$ parameters. This correlation has been validated with a series of 24 triols of known absolute configuration. Finally, the study shows how to distinguish the *pro-R* and *pro-S* methylene protons by simple examination of their vicinal coupling constants and relative chemical shifts. This finding is the first example in which the absolute configuration of a trifunctional compound has been determined by NMR spectroscopy.

Experimental Section

General esterification procedure: The tris-MPA esters **1–4**, **6–16**, **18–23, 26**, and **28** were obtained in solution with CH_2Cl_2 by treatment of the corresponding triol (1 equiv) with (*R*)- and (*S*)-MPA (4.5 equiv) in the presence of EDC (4.5 equiv) and DMAP (cat.). The reaction mixtures were stirred at room temperature for 24–48 h. The organic layers were washed with H_2O, HCl (1 M), H_2O, $NaHCO_3$ (sat.), and H_2O, dried over Na_2SO_4, and concentrated under reduced pressure (the acidic workup was omitted for triol **20**). The tris-MPA esters **5** and **17** were obtained from (*R*)- and (*S*)-MPA, EDC, and DMAP in dry MeCN at 40 °C for 24 h and hexakis-esters **24** from (*R*)- and (*S*)-methoxyphenylacetyl chloride (MPACl) in dry pyridine at room temperature for 30 h. After completion of the reactions, the solvents were evaporated, and the residues were diluted with CH_2Cl_2. Elaborations were performed following the same procedure as described above. Finally, purifications were performed by flash column chromatography on silica gel (230–400 mesh; hexane/AcOEt, 8:2 or 7:3), thus yielding the corresponding tris-MPA esters derivatives (80–95% yield after purification).

NMR spectroscopy: NMR spectra were recorded at 250 and 500 MHz (^{1}H nuclei) in $CDCl_3$ or CD_2Cl_2/CS_2 (1:4) for low-temperature ^{1}H NMR spectroscopic experiments. Chemical shifts (ppm) were internally referenced to the trimethylsilane (TMS) signal ($\delta = 0.00$ ppm for ^{1}H NMR spectra) and to the $CDCl_3$ solvent peak ($\delta = 77.0$ ppm for ^{13}C NMR spectra). The *J* coupling constants were recorded in Hz. 1D ^{1}H NMR spectra: size: 32 K, pulse length: 2.8 μs (30°), 16 acquisitions; 1D ^{13}C NMR spectra: size: 64 K, pulse length: 3.5 μs (30°), 1024 acquisitions; 2D COSY spectra: sequence: *D*1–90-*t*1–90-*t*2; relaxation delay: $D1 = 0.5$ s; pulse length: 8.5 μs (90°); 2D NOESY spectra: sequence: *D*1–90-*t*1–90-τ_{mix}-90-*t*2; relaxation delay: $D1 = 0.5$ s; mixing time (τ_{mix}): 0.5 s, pulse length: 8.5 ms (90°); TPPI-mode, NS = 64.

Computational methods: DFT calculations were performed to elucidate the conformational preferences of the tris-MPA esters of (2*R*,3*R*)- and (2*S*,3*R*)-propane-1,2,3-triols as model compounds. The geometries of the most relevant conformations of the tris-MPA esters selected from our experimental studies were optimized at the B3LYP/6–311+G(2d,p) level. The NMR spectroscopic calculations were carried out with the GIAO method.[22] All the calculations were performed with the Gaussian 98 series of programs.[16]

Acknowledgements

This research was supported by the Ministerio de Ciencia y Tecnología (CTQ2008–01110/BQU) and the Xunta de Galicia (PGIDIT-06PXIB209029PR). We also thank Bruker Española S.A., Centro de Supercomputación de Galicia (CESGA) and Yamakawa Chemical Industry (Japan). F.F. was supported in part by a MEC-Juan de la Cierva Post-Doctoral Fellowship. E.L. was supported in part by a USC Pre-Doctoral Fellowship.

[1] A. J. Dale, H. S. Mosher, *J. Am. Chem. Soc.* **1973**, *95*, 512–519.
[2] a) B. Trost, J. L. Belletire, S. Godleski, P. McDougla, J. M. Balkovec, *J. Org. Chem.* **1986**, *51*, 2370–2374; b) M. Adamczeski, E. Quiñoá, P. Crews, *J. Org. Chem.* **1990**, *55*, 240–242; c) I. Ohtani, T. Kusumi, Y. Kashman, H. Kakisawa, *J. Am. Chem. Soc.* **1991**, *113*, 4092–4096.
[3] a) T. J. Wenzel in *Discrimination of Chiral Compounds Using NMR Spectroscopy*, Wiley-Interscience, New Jersey, **2007**; b) J. M. Seco, E. Quiñoá, R. Riguera, *Chem. Rev.* **2004**, *104*, 17–117; c) J. M. Seco, E. Quiñoá, R. Riguera, *Tetrahedron: Asymmetry* **2001**, *12*, 2915–2925.
[4] a) I. Louzao, R. García, J. M. Seco, E. Quiñoá, R. Riguera, *Org. Lett.* **2009**, *11*, 53–56; b) F. Freire, E. Quiñoá, R. Riguera, *Chem. Commun.* **2008**, *35*, 4147–4149; c) S. Porto, J. M. Seco, E. Quiñoá, R. Riguera, *Org. Lett.* **2007**, *9*, 5015–5018; d) G. Uray in *Houben-Weyl Methods in Organic Chemistry, Vol. 1*, (Eds.: G. Helmchen, R. W. Hoffmann, J. Mulzer, E. Schaumann), Thieme, Stuttgart, New York, **1996**, p. 253; e) E. L. Eliel, S. H. Wilen, L. N. Mander, *Stereochemistry of Organic Compounds*, Wiley-Interscience, New York, **1994**, p. 221.
[5] a) R. T. Williamson, A. Boulanger, A. Vulpanovici, M. A. Roberts, W. H. Gerwick, *J. Org. Chem.* **2002**, *67*, 7927–7936; b) Sh. K. Latypov, J. M. Seco, E. Quiñoá, R. Riguera, *J. Am. Chem. Soc.* **1998**, *120*, 877–882.
[6] a) R. García, J. M. Seco, S. A. Vázquez, E. Quiñoá, R. Riguera, *J. Org. Chem.* **2006**, *71*, 1119–1130; b) Y. Yang, M. M. Kayser, D. Hooper, *Chirality* **2005**, *17*, 131–134; c) R. García, J. M. Seco, S. A. Vázquez, E. Quiñoá, R. Riguera, *J. Org. Chem.* **2002**, *67*, 4579–4589; d) J. M. Seco, L. H. Tseng, M. Godejohann, E. Quiñoá, R. Riguera, *Tetrahedron: Asymmetry* **2002**, *13*, 2149–2153; e) J. M. Seco, E. Quiñoá, R. Riguera, *Tetrahedron* **1999**, *55*, 569–584; f) B. López, E. Quiñoá, R. Riguera, *J. Am. Chem. Soc.* **1999**, *121*, 9724–9725.
[7] a) S. Porto, J. M Seco, J. F. Espinosa, E. Quiñoá, R. Riguera, *J. Org. Chem.* **2008**, *73*, 5714–5722; b) S. Porto, J. Durán, J. M. Seco, E. Quiñoá, R. Riguera, *Org. Lett.* **2003**, *5*, 2979–2982.
[8] a) F. Freire, F. Calderón, J. M. Seco, A. Fernández-Mayoralas, E. Quiñoá, R. Riguera, *J. Org. Chem.* **2007**, *72*, 2297–2301; b) F. Freire, J. M. Seco, E. Quiñoá, R. Riguera, *J. Org. Chem.* **2005**, *70*, 3778–3790; c) F. Freire, J. M. Seco, E. Quiñoá, R. Riguera, *Org. Lett.* **2005**, *7*, 4855–4858; d) F. Freire, J. M. Seco, E. Quiñoá, R. Riguera, *Chem. Eur. J.* **2005**, *11*, 5509–5522; e) S. Higashibayashi, Y. Kishi, *Tetrahedron* **2004**, *60*, 11977–11982; f) H. Fukui, Y. Fukushi, T. Tahara, *Tetrahedron Lett.* **2003**, *44*, 4063–4065. For others approaches for diols and polyols see: g) Seike, H.; Ghosh, I.; Kishi, Y. *Org. Lett.* **2006**, *8*, 3861–3864; h) Ghosh, I.; Kishi, Y.; Tomoda, H.; Omura, S. *Org. Lett.* **2004**, *6*, 4719–4722; i) Y. Kobayashi, N. Hayashi, Y. Kishi, *J. Am. Chem. Soc.* **2003**, *125*, 14379–14393; j) W. R. Hoffmann, U. Weidmann, *Chem. Ber.* **1985**, *118*, 3980–3992.
[9] a) V. Leiro, J. M Seco, E. Quiñoá, R. Riguera, *Org. Lett.* **2008**, *10*, 2729–2732; b) V. Leiro, J. M. Seco, E. Quiñoá, R. Riguera, *Org. Lett.* **2008**, *10*, 2733–2736; c) V. Leiro, F. Freire, J. M. Seco, E. Quiñoá, R. Riguera, *Chem. Commun.* **2005**, *44*, 5554–5556.
[10] See for instance: a) J. Boyer, Y. Allenbach, X . Ariza, J. Garcia, Y. Georges, M. Vicente, *Synlett* **2006**, *12*, 1895–1898; b) G.-L. Zhao, P. Dziedzic, I. Ibrahem, A. Córdova, *Synlett* **2006**, *20*, 3521–3524; c) D. J. Dixon, L. Krause; S. V. Ley, *J. Chem. Soc. Perkin Trans. 1* **1999**, *12*, 1627–1630; d) M. S. VanNieuwenhze, K. B. Sharpless, *Tetrahedron Lett.* **1994**, *35*, 843–846; e) T. Katsuki, A. W. M. Lee, P. Ma, V. S. Martin, S. Masamune, K. B. Sharpless, D. Tuddenham, F. J. Walker, *J. Org. Chem.* **1982**, *47*, 1378–1380.
[11] E. Lallana, F. Freire, J. M. Seco, E. Quiñoá, R. Riguera, *Org. Lett.* **2006**, *8*, 4449–4452.
[12] S. K. Latypov, J. M. Seco, E. Quiñoá, R. Riguera, *J. Org. Chem.* **1996**, *61*, 8569–8577.
[13] The same *sp/ap* conformational equilibria must be expected for the enantiomeric tris-MPA ester derivatives of the corresponding *syn* type B and *anti* type C triols.
[14] Conformer *gt*: H(2′) is oriented *gauche* to *pro-S* H and *trans* to *pro-R* H; conformer *tg*: H(2′) is oriented *trans* to *pro-S* H and *gauche* to *pro-R* H; conformer *gg*: H(2′) is oriented *gauche* to both *pro-S* H and *pro-R* H.
[15] G. Keck, D. Krishnamurthy, *J. Org. Chem.* **1996**, *61*, 7638–7639.
[16] H. C. Kolb, M. S. Van Nieuwenhze, K. B. Sharpless, *Chem. Rev.* **1994**, *94*, 2483–2547.
[17] Theoretical calculations were performed with Gaussian 98 (Revision A.7), M. J. Frisch, G. W. Trucks, H. B. Schlegel, G. E. Scuseria, M. A. Robb, J. R. Cheeseman, V. G. Zakrzewski, J. A. Montgomery, R. E. Stratmann, J. C. Burant, S. Dapprich, J. M. Millam, A. D. Daniels, K. N. Kudin, M. C. Strain, O. Farkas, J. Tomasi, V. Barone, M. Cossi, R. Cammi, B. Mennucci, C. Pomelli, C. Adamo, S. Clifford, J. Ochterski, G. A. Petersson, P. Y. Ayala, Q. Cui, K. Morokuma, D. K. Malick, A. D. Rabuck, K. Raghavachari, J. B. Foresman, J. Cioslowski, J. V. Ortiz, B. B. Stefanov, G. Liu, A. Liashenko, P. Piskorz, I. Komaromi, R. Gomperts, R. L. Martin, D. J. Fox, T. Keith, M. A. Al-Laham, C. Y. Peng, A. Nanayakkara, C. Gonzalez, M. Challacombe, P. M. W. Gill, B. G. Johnson, W. Chen, M. W. Wong, J. L.

Andres, M. Head-Gordon, E. S. Replogle and J. A. Pople, Gaussian, Inc., Pittsburgh PA, **1998**.

[18] The most relevant conformational processes are the modification of the *sp*/*ap* ratio and the rotation around the CO–C(1′) bond (i.e., conformers I–III).

[19] In the [*sp*-*gt*-II] conformer, the *pro*-*S* H atom resonates at lower field than the *pro*-*R* H atom, as the *pro*-*S* H and *pro*-*R* H atoms are shielded and deshielded, respectively, by the carbonyl group of the MPA auxiliary at C(1′) (see Figure 9a).

[20] In the [*sp*-*gt*-I] conformer, the anisotropic effects acting on the *pro*-*R* H and *pro*-*S* H atoms are very similar for both protons, thus resulting in very similar NMR resonances.

[21] Although the values of $\Delta\delta^{RS}$ for H(2′) of close to zero were obtained for compounds of an *anti* configuration, that is, **13**, **14**, **16**, **17**, **19**, and **21**–**24**, values clearly higher than zero were also observed (for **15**, **18**, and **20**); this apparent inconsistency can be easily explained because, due to the larger conformational freedom of the auxiliary at C(1′) than the auxiliary at C(3′), in these examples, the balance between both auxiliaries is shifted toward the MPA moiety at the secondary hydroxy group, with the contribution of this auxiliary being significantly larger than that of the other auxiliary, thus resulting in positive and negative $\Delta\delta^{RS}$ values of H(2′) in those *anti* type C and *anti* type D examples, respectively; it is important to note that when this occurs, the $|\Delta(\Delta\delta^{RS})|$ parameter is positively affected, with the difference between the $\Delta\delta^{RS}$ values of H(2′) and H(3′) becoming larger than expected.

[22] In fact, the sign of the $\Delta\delta^{RS}$ value for H(2′) is the opposite of that expected.

[23] J. R. Cheeseman, G. W. Trucks, T. A. Keith, M. J. Frisch, *J. Chem. Phys.* **1996**, *104*, 5497–5509.

[24] Signal overlap prevented the study of hexakis-ester **24**.

Received: June 3, 2009
Published online: September 23, 2009

